AIAA JOURNAL
Vol. 37, No. 2, February 1999

# Use of Fracture Mechanics and Shape Optimization for Component Designs

L. Gani* and S. D. Rajan†
*Arizona State University, Tempe, Arizona 85287*

**About half of mechanical failures are due to repeated loading. Most of the failures are fatigue related, and the fatigue problem has been of major concern in the design of structures. The failure is a function of, among other factors, the external loads, material behavior, geometry of the structure, and crack characteristics. The relationship between structural geometry and number of life cycles to failure is investigated to improve the fatigue life of structural components. The linear elastic fracture mechanics (LEFM) approach is integrated with shape optimal design methodology. The primary objective of the design problem is to enhance the life of the structure. The results from LEFM analyses are used in the fatigue model to predict the life of the structure before failure is deemed to have occurred. The shape of the structure is changed using the natural shape optimal design methodology. Gradient-based nonlinear programming techniques are used with the computed sensitivity information to predict the required shape changes. Relevant issues such as problem formulation, finite element modeling, mesh generation, and regeneration are discussed. Two design examples are solved, and the results show that, with proper shape changes, the life of structural systems subjected to fatigue loads can be enhanced significantly.**

## Introduction

ABOUT half of mechanical failures are due to repeated loading.[1] Most of the failures are fatigue related, and the fatigue problem has been of major concern in the design of structures. Engineers have been developing many approaches to deal with this problem. The majority of such investigations usually focus on the relationship between crack growth and response measures such as the applied stress range, strain range, and mean stress. This relationship characterizes fatigue life, which is defined as the total number of cycles or the time to induce fatigue damage and to initiate a dominant fatigue flaw that propagates to final failure.[2] An economic study estimated the cost of failures due to fracture in the United States in 1978 at $\$119 \times 10^9$ (in 1982 dollars) or about 4% of the gross national product.[3] This study estimated that if the current technology were applied the annual cost could be reduced appreciably and that further fracture mechanics research could reduce this figure by $\$28 \times 10^9$. Failures can be reduced, to a larger extent, through improved design practice.

Understanding the fatigue failure phenomenon is still an active area of research. The early research focused on discontinuities in the material to explain crack growth. Empirical relationships were developed, and the material constants in the expressions were usually obtained through experimental data. Research in the past two decades has shown that various factors, such as energy dissipation, early growth of short cracks, and friction, contribute to fatigue crack growth.[4–6] It should be noted that a crack growth is not independent of structural geometry. In this research, the relation between structural geometry and fatigue life is investigated by integrating the linear elastic fracture mechanics (LEFM) approach with shape optimal design optimization tools.[7] The major thrust of this paper is a discussion of the methodology aimed at improving the life of a structural system or component through appropriate design changes. Achieving this objective requires the understanding of fracture mechanics, material behavior, finite element analysis, geometric modeling, mesh generation, design optimization, and design principles, to name a few. There are three key issues that need to be dealt with to achieve the aforementioned objectives: an understanding of the LEFM approach, which provides the basis for computing the fatigue life of a structural system; the design problem formulation that is necessary to solve the problem with the available optimization methodologies; and finite element modeling and analysis needed to compute the LEFM parameters. The rest of the paper deals with these three topics, with the primary focus on the latter two topics.

## Problem Formulation

For practical structures, it is either impossible or prohibitively expensive to design structural systems for life without fatigue failure. A better alternative is to design with the viewpoint of meeting the cost and performance requirements of a structural system while maximizing the life of the system. One could also design to achieve a certain minimum life while minimizing the design, manufacturing, and maintenance costs. In any case, the design problem can be posed as an optimal design problem. Such a problem, which is solved using a mathematical programming technique, is usually stated as follows:

$$\text{find} \quad \boldsymbol{b} \in R^k$$

$$\text{to maximize} \quad \{f(\boldsymbol{b}): \boldsymbol{g}(\boldsymbol{b}), \boldsymbol{b}^L \le \boldsymbol{b} \le \boldsymbol{b}^U, \Gamma(\boldsymbol{b}) \in V\} \qquad (1)$$

where $\boldsymbol{b}$ is the vector of design variables, $f(\boldsymbol{b})$ is the objective function, $\boldsymbol{g}(\boldsymbol{b})$ are the constraint functions, $\boldsymbol{b}^L$ and $\boldsymbol{b}^U$ are the lower and upper bounds on the design variables, and $\Gamma$ belongs to a class $V$ that is sufficiently smooth and satisfies design needs. The objective function in this study is to maximize the number of life cycles $N$ that is a function of stress intensity factors $K$ and crack length $a$. The constraints deal with the performance of the system and include, among other things, the limits on stresses and displacements. With the problem at hand, there are several issues to be resolved before a conventional optimization technique can be used to solve the design problem.

### Computation of the Objective Function

The objective function has to be modified so that the formulation follows the standard nonlinear programming (NLP) format. Because the primary objective of the design exercise is to maximize the life of the structure (with an existing crack), the objective function in this formulation is the number of cycles to failure that is given as

$$N = N_0 + \sum_{i=1}^{n} \Delta N_i, \qquad i = 1, 2, 3, \ldots, n \qquad (2)$$

Received April 14, 1998; revision received Sept. 1, 1998; accepted for publication Sept. 28, 1998. 

*Graduate Assistant, Department of Civil Engineering; currently Senior Engineer, Structural Analysis, BPPT, Jakarta, Indonesia.
†Professor, Department of Civil Engineering. Member AIAA.

where $N_0$ is the initial number of cycles (due to initial crack), $\Delta N_i$ is the number of cycles required to obtain crack extension $i$, and $n$ is the number of crack extensions to failure. Failure is defined as the state of the system with a single crack that prevents the structure from performing as required. The computation of $\Delta N_i$ is based on modified Paris law[8,9] for mixed-mode fatigue crack growth.[10] The relationship for crack growth rate is given as

$$\frac{da}{dN} = n(\Delta K_v)^c \tag{3}$$

where $n$ and $c$ are material constants obtained experimentally and $a$ is the crack length. In addition,

$$\Delta K_v = \tfrac{1}{2}\left[\Delta K_I + \sqrt{\left(\Delta K_I^2 + \Delta K_{II}^2\right)}\right]$$
$$\Delta K_I = K_{I\max} - K_{I\min}, \qquad \Delta K_{II} = K_{II\max} - K_{II\min} \tag{4}$$

where $K_I$ and $K_{II}$ are the stress intensity factors (SIF) corresponding to mode I and II deformations, respectively, and $\Delta K$ measures the range in the SIF values. Based on the concept that during compression loading the crack closes and, hence, no stress intensity factor $K$ can exist, fatigue crack growth data usually refer to the tension condition. In other words, the compression loads have little influence on crack growth behavior. With this assumption, constant amplitude loading and ambient temperature, Eq. (3) can be rewritten as

$$\frac{da}{dN} = n(K_{v\max})^c \tag{5}$$

where

$$K_v = \tfrac{1}{2}\left[K_I + \sqrt{\left(K_I^2 + K_{II}^2\right)}\right] \tag{6}$$

Assuming that the crack increment $\Delta a$ is small with respect to the geometry of the structure, the SIF can be approximated as piecewise linear functions $K = K(a)$, and $\Delta N_i$ can be computed as follows[11]:

$$\int dN = \Delta N = \int \frac{da}{nK_{v\max}^c} \tag{7}$$

with $K = K(a) = ma + b$. Equation (7) can be expressed as

$$\Delta N = \frac{1}{n}\int (ma + b)^{-c}\, da \tag{8}$$

$$\Delta N = \frac{1}{n(1-c)m}(ma + b)^{1-c} \tag{9}$$

$$\Delta N = \frac{1}{n(1-c)m}\left(K_1^{1-c} - K_0^{1-c}\right) \tag{10}$$

where $K_0$ is the value of $K_{v\max}$ at the start of the increment, $K_1$ is the value of $K_{v\max}$ at the end of the increment, and $m$ is the slope of the line defined as

$$m = \frac{K_1 - K_0}{a_1 - a_0} = \frac{K_1 - K_0}{\Delta a} \tag{11}$$

Hence, Eq. (2) can be computed.

**Avoiding Premature Convergence**

If the change in the geometry of the structure is very small, there is a possibility that the new value of $N$ is the same (because the crack length and the crack path may not change). The implication is that this condition may result in the gradient of objective function being zero. Hence, to avoid premature convergence, the volume of the structure is inserted as an additional term in the objective function. Equation (1) can be rewritten as

$$\text{find} \quad \boldsymbol{b} \in R^k \text{ to}$$
$$\min \quad \{\bar{f}(\boldsymbol{b}): \boldsymbol{g}(\boldsymbol{b}), \boldsymbol{b}^L \le \boldsymbol{b} \le \boldsymbol{b}^U, \Gamma(\boldsymbol{b}) \in V\} \tag{12}$$

where $\bar{f}(\boldsymbol{b})$ is the modified objective function expressed as

$$C_1 V(\boldsymbol{b}) - C_2 N(a, K) \tag{13}$$

where $C_1$ and $C_2$ are (adjustable) weighting factors, $V(\boldsymbol{b})$ is the volume of the structure, and $N(a, K)$ is the total number of cycles to failure. Experience has shown that the modified objective function plays a very important role in the stability and convergence of the design problem. As shown in the Numerical Examples section, it is also possible to impose the amount of material to be used as a constraint. This constraint forces the optimizer to redistribute the material to increase the life of the system.

**Imposition of the Constraints**

The imposition of the element-related constraints, such as a stress constraint, requires special attention. This is because the mesh dynamically changes as the crack propagates. Hence, the stress constraint cannot be imposed elementwise. There are three possible solutions. First, the stress constraints can be imposed nodewise. Because the mesh changes, the nodal stress constraint can be imposed only at those predetermined points that remain as mesh nodes. In addition, one would have to guess where the maximum stress measure might occur. Second, the stress constraint can be imposed patchwise. In other words, the maximum stress can be computed over all of the elements in a patch and can be used as the stress constraint. Experience has shown that for certain problems convergence is difficult to obtain because the maximum stress measure, e.g., von Mises, can oscillate with changing meshes. Third, instead of imposing a stress constraint, the stress measure can be used as a stopping criterion during the crack propagation analysis. This is the strategy used in the current study. Similar comments also apply to nodal displacement constraints.

## Finite Element Modeling

Critical to the process of carrying out the crack propagation analysis using the finite element method are the issues of generating the structural model, mesh generation, and mesh regeneration associated with a moving crack tip. Whereas the literature is replete with papers and books that discuss LEFM-based finite element analysis[12–18] and different approaches to the problem of mesh generation, literature that deals with model and mesh regeneration associated with crack propagation is very limited.[11,19] Whereas manual controls or user input are sometimes necessary, in a situation involving crack propagation or shape optimal design, it is desirable to minimize (or eliminate) user intervention as much as possible. Semiautomatic (or automatic) mesh generation under these conditions is possible if the mesh generation is somehow linked to the model representation scheme. A mesh generator called AUTOMESH[20] has been modified to handle the requirements of the current research. Issues specific to handling the crack propagation problem are discussed in the next few paragraphs. Details of the mesh generator can be found in a prior publication.[21]

One of the preferred schemes for automatic mesh generation is to provide the user with selective control parameters that affect the mesh density and provide a smooth mesh transition. In addition, it should be noted that, with crack propagation and shape optimal design, the choice of remeshing scheme becomes very important. If local remeshing is used, then consideration must be given to maintaining compatibility between the existing mesh and the area to be remeshed. For example, the mesh density requirement differs greatly between the region around a crack tip and the rest of the structure.

In this research, the structural model is defined using the cell decomposition scheme.[22] The model is essentially divided into two or more patches that are glued to each other on the sides shared by two patches. A patch is defined as a continuous domain where the material and thickness properties remain the same. Crack initiation and subsequent extension is restricted to one patch. The restriction was imposed because of data handling issues in the computer program more than any other reason. Patch remeshing (a subset of the global remeshing scheme) is adopted in this research for several reasons. First, storage space (memory) requirements are minimal. By remeshing a patch that has a crack in it, the maximum storage space required for the patch is no more than three times the original

storage space for the patch. Second, the characteristics of automatic mesh generation, AUTOMESH, are preserved without the introduction of additional strategies to handle special situations. Third, the compatibility between adjacent patches is automatically maintained because only the interior of the patch containing the crack is remeshed. Fourth, additional user intervention or input is not required during remeshing. The next two subsections focus on patch remeshing.

**Element Deletion Scheme**

Because patch remeshing is carried out instead of global remeshing during crack propagation, the efficiency of the element deletion scheme is very important. The following steps are used in the implementation:

1) Before removing elements around a crack tip, information related to the crack tip is saved, e.g., material and thickness properties. The patch information is later regenerated and includes the original boundary and the crack-related information.

2) The crack-related information includes the crack locus, redefinition of the crack tip node, and crack boundary nodes. The previous crack tip is defined as the crack boundary nodes after the first crack increment and the creation of the crack tip. Care is taken to redefine the moving crack boundary by minimizing the number of straight line segments defining the crack surface.

Once these pieces of information are saved and all data structures influenced by nodes and elements are updated, remeshing of the patch can take place.

**Remeshing Strategy**

The remeshing strategy includes three distinct preprocessing steps. These steps are implemented before AUTOMESH is called to remesh the patch.

*Creation of Rosette Elements*

Rosette elements are defined as individual elements around a crack tip that cluster together like a rosette. The elements are singular finite elements with the midside nodes set at quarter-points of the length of the element side. These elements are required to compute SIF $K$. Several researchers have investigated the effect of the size of singular elements in predicting the SIF. Harrop[14] indicated that the singular elements can represent the stress singularity and constant finite stress term only. To ensure accurate stress predictions, the size of the singular elements must be selected appropriately. In this research, the ratio of crack tip element size with respect to the crack length is initially set equal to 0.50 with user overrides available if necessary. This value, called the rosette ratio (RR), is not a constant and is dynamically updated. Let the element ratio (ER) be defined as the ratio of the size of the rosette element to the size of the smallest element in the rest of the patch, $E_{\min}$. If

$$r > 2 \times \mathrm{ER} \times E_{\min} \tag{14}$$

then

$$\mathrm{RR} = \max\left(1.0, \frac{2 \times \mathrm{ER} \times E_{\min}}{D_l}\right) \tag{15}$$

where the default value of ER is set to 1.0 and

$$r = \mathrm{RR} \times D_l$$

where $D_l$ is the distance from current crack tip node to the node at crack boundary. On the other hand, if

$$r < \mathrm{ER} \times E_{\min} \tag{16}$$

then

$$\mathrm{RR} = \frac{\mathrm{ER} \times E_{\min}}{D_l} \tag{17}$$

Finally, the maximum of the RR values obtained from the preceding equations is used. The major driving force here is to obtain crack tip elements with the proper aspect ratio.

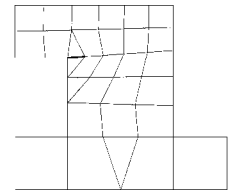

**Fig. 1 Initial mesh.**

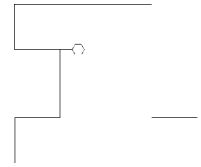

**Fig. 2 Creation of element rosette.**

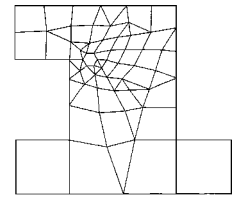

**Fig. 3 Remeshing using AUTOMESH.**

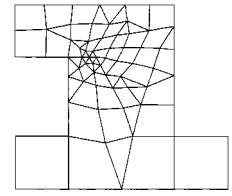

**Fig. 4 Final mesh including the rossette elements.**

*Mesh Density Coefficients*

Because rosette elements are created independently, compatibility has to be maintained between the elements outside and inside the rosette and to provide a smooth mesh transition. The mesh density coefficient (MDC) values are computed for the nodes in the rosette to take care of this problem. First, the minimum value of MDC is taken as 0.1. Second, by assuming that the largest size of the rosette elements is less than or same as the smallest element size in the patch, one can then take the MDC value of the rosette nodes as being no more than the $\mathrm{MDC}_{\min}$ of the rest of the nodes in the patch. In other words,

$$C_r = \frac{E_{\mathrm{ros}}}{E_{\min}} = \frac{\mathrm{RR} \times D_l}{E_{\min}} \tag{18}$$

where $E_{\mathrm{ros}}$ is size of the rosette's elements and $C_r$ is the intermediate MDC. If $C_r$ is less than 0.1, then $C_r$ is equal to the user-specified minimum. On the other hand, if $C_r$ is greater than 1.0, then $C_r = 1.0$. Finally,

$$\mathrm{MDC}_{\mathrm{ros}} = C_r \times \mathrm{MDC}_{\min} \tag{19}$$

The major driving force here is to obtain a smooth mesh transition from the rosette elements to the rest of the patch.

*Subgrid Creation*

Finally, the split line connecting the crack tip to the patch boundary has to be created. Once $\mathrm{MDC}_{\mathrm{ros}}$ has been computed, the next step is to compute internal points between the last crack tip and the current crack tip. The internal nodes on these lines are created in the same way as the internal nodes on a split line. The next step is to invoke AUTOMESH to remesh this region. The sequence of steps for an illustrative example is shown in Figs. 1–4.

## Numerical Examples

Two design problems are solved to illustrate the developed design methodology. The natural shape optimal design methodology[23–25] is used to solve both of the problems. The method of feasible directions[26,27] is used as the optimizer. The design sensitivity information is computed using the forward difference method.

**Table 1 Data for cantilever beam**

| Item | Value |
|---|---|
| Modulus of elasticity $E$ | 1.05 ($10^7$) psi |
| Uniform load $p$ | 750 psi |
| Poisson ratio $\nu$ | 0.33 |
| Thickness $t$ | 0.036 in. |
| Material toughness $K_{ic}$ | 140 ksi $\sqrt{}$in. |
| Allowable (von Mises) stress $\bar{\sigma}$ | $10^5$ psi |
| Plate width $L$ | 20 in. |
| Plate height $h$ | 10 in. |
| Initial crack length $a$ | 1 in. |

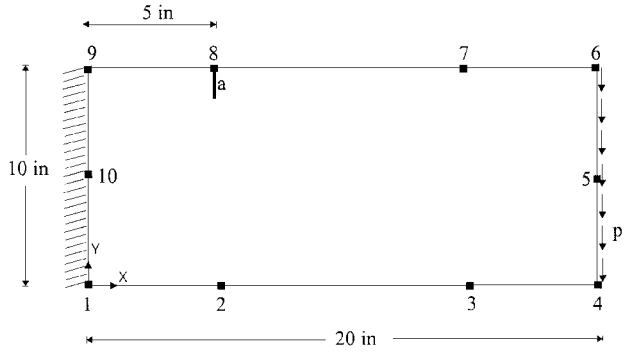


**Fig. 5 Model of the cantilever beam with an initial crack.**

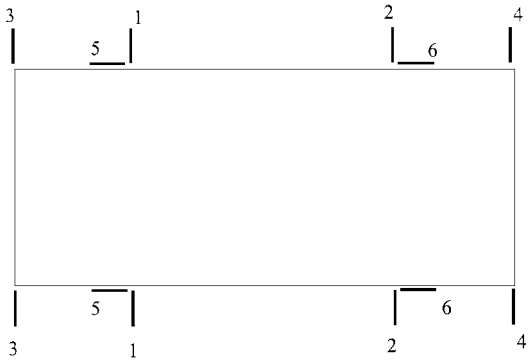


**Fig. 6 Six design variables associated with specified displacements of the key points.**

**Table 2 Initial and final design details**

| | Initial coordinate | | Final coordinate | |
|---|---|---|---|---|
| Node | $X$, in. | $Y$, in. | $X$, in. | $Y$, in. |
| 1 | 0.0 | 0.0 | 0.0 | −2.22 |
| 4 | 20.0 | 0.0 | 20.0 | 2.36 |
| 6 | 20.0 | 10.0 | 20.0 | 7.64 |
| 9 | 0.0 | 10.0 | 0.0 | 12.22 |
| $N$ | 14 | | 434 | |

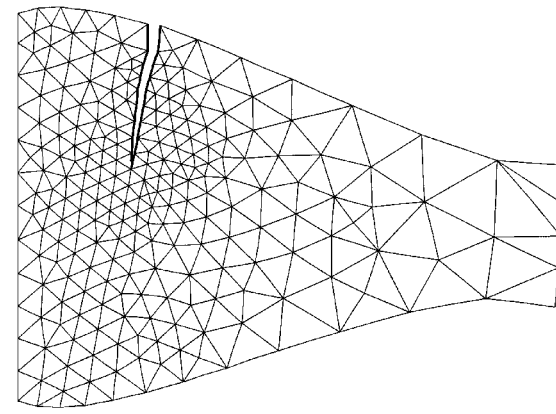

**Fig. 7 Final mesh and shape with exaggerated displacements.**

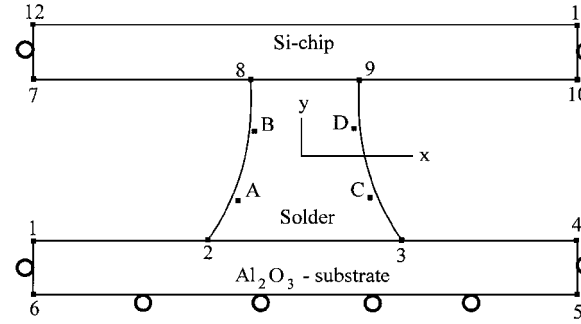


**Fig. 8 Solder joint model and boundary conditions.**

**Cantilever Beam with Shear Loads**

The first example is a cantilever beam with the shear loads at one end and fixed at the other end. This is a plane stress problem. The initial shape is shown in Fig. 5. The problem data are given in Table 1.

The problem domain is made up of one patch defined by four straight lines (1–10, 10–9, 4–5, 5–6) and two cubic Bezier curves (1–2–3–4, 6–7–8–9). The cubic Bezier curves are used to define shape change on the top and bottom sides. Six design variables are used and are related to the displacements of the Bezier key points, as shown in Fig. 6. Design variable linking is used to maintain structural symmetry about the $x$ axis.

The objective of this example is to maximize the life of the structure through shape changes. The number of cycles is computed using the Paris law, with the coefficients $A = 28.0$ and $n = 4.9$. The initial number of cycles $N_0$ is set to zero. The objective function is taken as Eq. (13) with $C_1 = 1.0$ and $C_2 = 10.0$. These constants were selected to favor enhancing the life of the structure over the usage of the material. The limit on the latter was placed through a volume constraint of 10 in.$^3$. The other constraints for this problem include geometric constraints that limit the extent of the structure in the $y$ direction. The von Mises failure criterion is not directly used as a constraint; instead, it is used as a stopping criterion in the crack propagation analysis. Also the maximum displacement at a node in the $x$–$y$ directions is limited to 1% of the dimension of the structure in that direction: in other words, 0.1 in. in the $y$ direction and 0.2 in. in the $x$ direction.

The final results were obtained in 15 design iterations. The number of cycles to failure was increased to 434 from 14 by making the appropriate shape changes. During the course of the design, the finite element analysis was carried out 120 times (gradient plus line search). The final results are shown in Fig. 7 and Table 2. As is seen in this example (as well as the next), the shape changes take place so as to shift more material in a manner that makes the structure stiffer and reduces the SIF at the crack tip. In this regard, the location and the size of the initial crack determine the final solution.

**Flip Chip Solder Joints**

The second example is the design of a flip chip solder joint under thermal loading.[28] Whereas the entire package is made up of tens of these solder joints, experience has shown that the corner joints are the most vulnerable. Hence, analyzing and understanding the behavior of a typical corner joint is crucial to the design of the package. The structural model for such an analysis is shown in Fig. 8. The top material is an Si chip with a coefficient of thermal expansion (CTE) $\alpha = 2.4 \times 10^{-6}/^\circ$C. The bottom portion is $Al_2O_3$ substrate with $\alpha = 6.5 \times 10^{-6}/^\circ$C. The middle part is the 5 wt% Sn 95 wt% Pb solder with $\alpha = 28.7 \times 10^{-6}/^\circ$C. Stresses are induced in the package due to CTE mismatch between the different components. The problem domain is divided into three patches, one for each material or component. The patch containing the solder is defined by two straight lines and two cubic Bezier curves. The chip and the substrate are modeled with patches defined by six straight lines. The

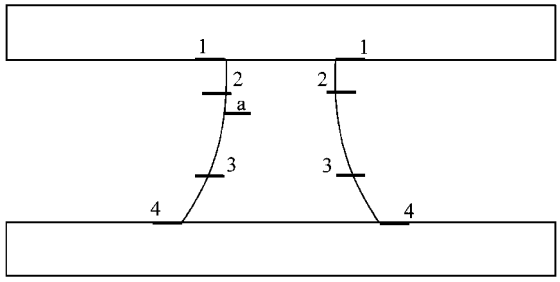


**Fig. 9 Initial crack and design variables.**

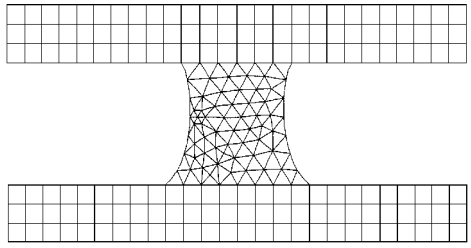

**Fig. 10 Initial mesh and shape (case A).**

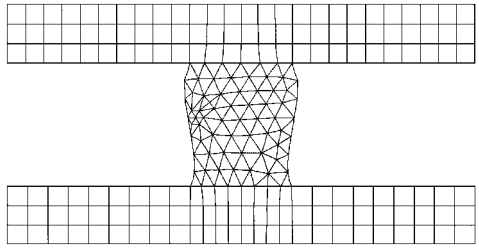

**Fig. 11 Final mesh and shape (case A).**

design variables used in this problem are four groups of specified displacements, as shown in Fig. 9. The choice of the design variables is such that the solder is symmetric about the $y$ axis and the height of the solder does not change (a package requirement).

The intent of this example is to study the effect of shape change (in a solder with a single existing crack) on the number of life cycles. The solder joint has the following properties: Young's modulus $E = 2600$ MPa, Poisson's ratio $\nu = 0.3$, allowable stress $\bar{\sigma} = 100$ MPa, and critical toughness $K_{IC} = 8$ MPa $\sqrt{\text{mm}}$. The entire package is assumed to have a uniform temperature change $\Delta T = 2000^{\circ}$C during temperature loading. The number of cycles is computed using Paris law ($\mathrm{d}a/\mathrm{d}N = A \times \Delta K^n$) with the coefficients $A = 2.77 \times 10^{-7}$ and $n = 3.26$ (Ref. 28). Finally, the thermal fatigue life $N_f$ of the corner solder joint is equal to $\lambda N$, where $\lambda = 0.00078$ is a thermal stress correction factor.[28]

The initial crack is 0.02 mm and is located on the upper-left-hand side of solder joint (a in Fig. 9). With the initial concave shape, the number of cycles to failure $N$ is 9937, with a corresponding crack length of 0.10 mm. On convergence (with the final shape), $N$ is increased to 14,520, with a corresponding crack length of 0.10 mm. After four iterations (or 25 function evaluations), the life of the solder joint increases by 4583 or about 46.1%. The final and initial dimensions are presented in Table 3. The initial and the final shapes are shown in Figs. 10 and 11. This study is case A (Table 3 and Figs. 10 and 11).

To ensure that the convergence is not premature, the model is rerun using a different initial shape. Case B starts with a convex shape for the solder. The results show that the objective function and the final shape for case B are very close to the results from case A. The initial and final shapes for case B are shown in Figs. 12 and 13, respectively.

One should be careful in interpreting the problem formulation and results. Normally cracks occur at the interfaces, e.g., die or substrate. In this example, the existing crack is below the interface. This is the location at which the probability of occurrence

**Table 3 Initial and final dimensions (case A)**

| | Initial coordinate | | Final coordinate | |
|---|---|---|---|---|
| Node | $X$, mm | $Y$, mm | $X$, mm | $Y$, mm |
| 1 | −0.60 | 0.0 | −0.60 | 0.0 |
| 2 | −0.19 | 0.0 | −0.13 | 0.0 |
| 3 | 0.19 | 0.0 | 0.13 | 0.0 |
| 4 | 0.60 | 0.0 | 0.60 | 0.0 |
| 5 | 0.60 | −0.15 | 0.60 | −0.15 |
| 6 | −0.60 | −0.15 | −0.60 | −0.15 |
| 7 | −0.60 | 0.32 | −0.60 | 0.32 |
| 8 | −0.15 | 0.32 | −0.13 | 0.32 |
| 9 | 0.15 | 0.32 | 0.13 | 0.32 |
| 10 | 0.60 | 0.32 | 0.60 | 0.32 |
| 11 | 0.60 | 0.47 | 0.60 | 0.47 |
| 12 | −0.60 | 0.47 | −0.60 | 0.47 |
| A | −0.13 | 0.13 | −0.14 | 0.13 |
| B | −0.13 | 0.23 | −0.13 | 0.23 |
| C | 0.13 | 0.13 | 0.14 | 0.13 |
| $D$ | 0.13 | 0.26 | 0.13 | 0.23 |
| $N$ | 9,937 | | 14,520 | |

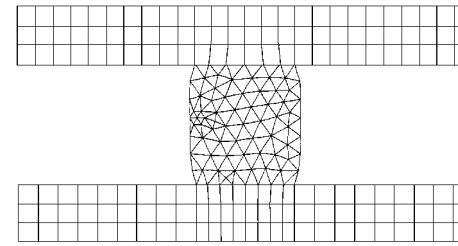

**Fig. 12 Initial mesh and shape (case B).**

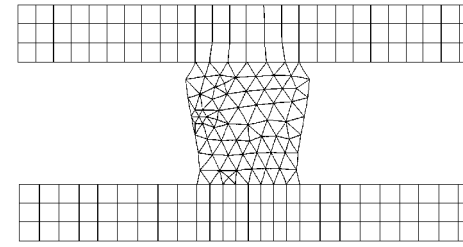

**Fig. 13 Final mesh and shape (case B).**

of the initial crack is the highest (possibly due to the flaw distribution during the formation of the solder) and is confirmed experimentally.[28] The optimal design results are also counter to the previously established observation that barrel-shaped solder joints have a shorter life compared to a more flexible hyperbolic shape.[29] However, in this design example, with the existing crack, the material redistribution is such that the solder is strengthened around the crack.

## Concluding Remarks

The relation between structural geometry and fatigue life $N$ has been developed by integrating LEFM with design optimization tools. The integrated design system uses design sensitivity analysis, a gradient-based optimizer, the finite element method with quarter-point elements in the vicinity of a crack tip, and a specially developed general two-dimensional mesh generator. Paris law is used to predict the life of the structural system and uses the developed relation between crack growth $\mathrm{d}a/\mathrm{d}N$ vs the applied SIF range $\Delta K$.

The problem formulation is the most crucial component for a variety of reasons. The use of standard gradient-based NLP techniques dictates that the problem statement be in the standard format. However, because of the traits of the problem, special changes are necessary to obtain a solution and speed up the convergence. The major requirement is that the objective function be sufficiently sensitive even to the smallest of changes in the design variables. This is necessary to avoid premature convergence. Also, instead of imposing the stress constraints, the failure criterion is used as

one of the stopping criteria during the crack propagation analysis. This approach overcomes the stability and convergence problems associated with other techniques of handling the stress (or displacement) constraints. The convergence for both the problems was quite rapid and smooth. On an average, between two and three function evaluations were necessary during line search.

Although the numerical examples show that the proposed methodology has tremendous potential, several deficiencies exist. Some of the improvements that can be made include the following: handling elasto–plastic fracture mechanics, other crack geometry (multiple cracks, interior cracks, etc.), and computing the gradients semianalytically.

## Acknowledgment

The authors wish to thank Ben Nagaraj, Motorola, for his invaluable comments and suggestions.

## References

[1]Fuchs, H. O., and Stephens, R. I., *Metal Fatigue in Engineering*, Wiley, New York, 1980, Chap. 1.

[2]Suresh, S., *Fatigue of Materials*, Cambridge Univ. Press, Cambridge, England, UK, 1991, Chaps. 1, 2.

[3]Duga, J. J., Fisher, W. H., Buxbaum, R. W., Rosenfield, A. R., Burh, A. R., Honton, E. J., and McMillan, S. C., "The Economic Effects of Fracture in the United States," National Bureau of Standards Special Publication 647-2, U.S. Dept. of Commerce, Washington, DC, March 1983.

[4]Faanes, S., and Fernando, U. S., "Influence of Contact Loading on Fretting Fatigue Behaviour," *Fatigue Engineering Material Structure*, Vol. 17, No. 8, 1994, pp. 939–947.

[5]Jono, M., and Song, J., "Growth and Closure of Short Fatigue Cracks," *Current Research on Fatigue Cracks*, Elsevier Applied Science, New York, 1987, pp. 41–65.

[6]Kaleta, J., and Zietek, G., "Representation of Cyclic Properties and Hysteresis Energy in $\alpha$-Brass Using a Certain Class of Elastic–Plastic Models," *Fatigue Engineering Material Structure*, Vol. 17, No. 8, 1994, pp. 919–930.

[7]Gani, L., "Prolonging Fatigue Life of Structural Components," Ph.D. Thesis, Dept. of Civil Engineering, Arizona State Univ., Tempe, AZ, May 1996.

[8]Paris, P. C., and Erdogan, F., "A Critical Analysis of Crack Propagation Laws," *Journal of Basic Engineering*, Vol. 85, No. 4, 1963, pp. 528–538.

[9]Paris, P. C., and Sih, G. C., "Stress Analysis of Cracks," American Society of Testing and Materials, ASTM STP 381, Jan. 1965, pp. 30–81.

[10]Henn, K., Richard, H. A., and Linnig, W., "Fatigue Crack Growth Under Mixed Mode and Mode II Cyclic Loading," *Proceedings of the 7th European Conference on Fracture*, edited by E. Czoboly, European Microbeam Analysis Society, Antwerp-Wilrijk, Belgium, 1988, pp. 1104–1113.

[11]Potyondy, D. O., Wawrzynek, P. A., and Ingraffea, A. R., "An Algorithm to Generate Quadrilateral or Triangular Element Surface Meshes in Arbitrary Domains with Applications to Crack Propagation," *International Journal of Numerical Methods in Engineering*, Vol. 38, No. 4, 1995, pp. 2677–2701.

[12]Barsoum, R. S., "On the Use of Isoparametric Finite Elements in Linear Fracture Mechanics," *International Journal of Numerical Methods in Engineering*, Vol. 10, No. 1, 1976, pp. 25–35.

[13]Chan, S. K., Tuba, I. S., and Wilson, W. K., "On the Finite Element Method in Linear Fracture Mechanics," *Engineering Fracture Mechanics*, Vol. 2, No. 1, 1970, pp. 1–17.

[14]Harrop, L. P., "The Optimum Size of Quarter-Point Crack Tip Element," *International Journal for Numerical Methods in Engineering*, Vol. 17, No. 3, 1982, pp. 1101–1103.

[15]Henshell, R. D., and Shaw, K. G., "Crack Tip Finite Elements Are Unnecessary," *International Journal of Numerical Methods in Engineering*, Vol. 9, No. 2, 1975, pp. 495–507.

[16]Reimers, P., "Simulation of Mixed Mode Fatigue Crack Growth," *Computers and Structures*, Vol. 40, No. 2, 1991, pp. 339–346.

[17]Saoma, V. E., and Schwemmer, D., "Numerical Evaluation of the Quarter-Point Crack Tip Element," *International Journal of Numerical Methods in Engineering*, Vol. 20, No. 9, 1984, pp. 1629–1641.

[18]Shih, C. F., "Relationship Between the J-Integral and the Crack Opening Displacement for Stationary and Extending Cracks," *Journal of the Mechanics and Physics of Solids*, Vol. 29, No. 4, 1981, pp. 305–326.

[19]Miyamoto, H., Fukuoa, S., and Kageyama, K., "Finite Element Analysis of Crack Propagation Under Compression," *Proceeding ICF4* (Waterloo, ON, Canada), Vol. 3, International Congress of Fracture, 1977, pp. 491–499.

[20]Budiman, J., "The Natural Shape Optimal Design Method with Adaptive Mesh Generation," Ph.D. Thesis, Dept. of Civil Engineering, Arizona State Univ., Tempe, AZ, May 1990.

[21]Rajan, S. D., Budiman, J., and Gani, L., "Topologically Based Adaptive Mesh Generator for Shape Optimal Design," *Proceedings of the AIAA/ASCE/ASME/AHS 32nd Structures, Structural Dynamics, and Materials Conference* (Baltimore, MD), Pt. 1, AIAA, Washington, DC, 1991, pp. 653–663.

[22]Mortenson, M. E., *Geometric Modelling*, Wiley, New York, 1985, Chaps. 2, 3.

[23]Belegundu, A. D., and Rajan, S. D., "A Shape Optimization Approach Based on Natural Design Variables and Shape Function," *Computer Methods in Applied Mechanics and Engineering*, Vol. 66, 1988, pp. 87–106.

[24]Rajan, S. D., and Belegundu, A. D., "Shape Optimal Design Using Fictitious Loads," *AIAA Journal*, Vol. 27, No. 1, 1989, pp. 102–116.

[25]Rajan, S. D., and Gani, L., "A Comparison of Natural and Geometric Approaches for Shape Optimal Design," *Proceedings of the AIAA/ASCE/ASME/AHS 31st Structures, Structural Dynamics, and Materials Conference* (Long Beach, CA), Pt. 1, AIAA, Washington, DC, 1990, pp. 196–205.

[26]Vanderplaats, G. N., and Moses, F., "Structural Optimization by Methods of Feasible Directions," *Journal of Computers and Structures*, Vol. 3, 1973, pp. 739–755.

[27]Zoutendijk, G., *Methods of Feasible Directions*, Elsevier, Amsterdam, 1960.

[28]Lau, J. H., and Rice, D. W., "Thermal Fatigue Life Prediction of Flip Chip Solder Joints by Fracture Mechanics Method," *Proceedings of the Joint ASME/ISME Conference on Electronic Packaging* (Milpitas, CA), American Society of Mechanical Engineers, New York, 1992, pp. 385–392.

[29]Ikegami, K., "Some Topics of Mechanical Problems in Electronic Packaging," *Proceedings of the Joint ASME/ISME Conference on Electronic Packaging* (Milpitas, CA), American Society of Mechanical Engineers, New York, 1992, pp. 567–573.

A. D. Belegundu
*Associate Editor*